

RESEARCH AND EDUCATION

Influence of object translucency on the scanning accuracy of a powder-free intraoral scanner: A laboratory study



Hong Li, PhD,^a Peijun Lyu, DDS, PhD,^b Yong Wang, MS,^c and Yuchun Sun, DDS, PhD^d

Intraoral scanning technology marks the beginning of a new era of fully digital dental processing. Direct optical surveying of intraoral structures is now being widely tested as a clinical alternative to conventional impression making.¹⁻⁴

Clinically, intraoral tissues and many different dental materials are translucent. When light encounters a translucent object, some light is reflected at the surface, some is scattered inside the object, and some is transmitted. Moreover, some of the scattered light exits the surface again, some is absorbed within the object, and some finally passes through the object.⁵ Subsurface scattering (SSS) refers to the phenomenon by which light scattered within an

ABSTRACT

Statement of problem. Limited information is available regarding the influence of object translucency on the scanning accuracy of a powder-free intraoral scanner.

Purpose. The purpose of this in vitro study was to evaluate the scanning accuracy of a confocal microscopy principle powder-free intraoral scanner on ceramic copings and to analyze the relationship between scanning accuracy and object translucency.

Methods. Six slice specimens (12×10 mm) and 6 offset copings (1.00-mm thickness) were made from different translucent homogeneous ceramic blocks (CEREC Blocs, S0-M to S5-M, highest to lowest translucency). The primary sintered zirconia offset coping was produced in the same way as the control. Optical parameters related to the translucency of each slice were measured with a spectrophotometer. Three-dimensional (3D) datasets of the surface morphology of offset copings were obtained by using the intraoral scanner. The same white wax resin bases were used for registration. Quantitative parameters of scanning trueness and precision were measured. One-way ANOVA was used to analyze the values of each parameter among the 6 ceramic blocks. Bivariate correlation was used to analyze the relationships between each parameter of scanning accuracy and translucency ($\alpha=.05$).

Results. Translucent copings showed a positive 3D bias (S0-M to S5-M: 0.149 ±0.038 mm to 0.068 ±0.020 mm), a narrower collar diameter (Dd=-0.067 mm), larger convergence angle ($\Delta\Phi=2.79$ degrees), and larger curvature radius of the internal gingivoaxial corner ($\Delta\rho=0.236$ mm). The smaller the percentage sum of scattering and absorption, the greater was the occurrence of scanning bias ($r=-0.918$) and curvature ($r=-0.935$) decrease.

Conclusions. Use of the tested powder-free intraoral scanner, higher translucency objects (greater translucency than S1-M/A1C) resulted in lower scanning accuracy and morphological changes. Therefore, more suitable methods of measurement are still required. (J Prosthet Dent 2017;117:93-101)

Supported by National High Technology Research and Development Program ("863" Program) of China grant 2013AA040802 and by National Natural Science Foundation of China grant 51475004.

^aGraduate student, Graduate Prosthodontics, Center of Digital Dentistry, Department of Prosthodontics, Peking University School and Hospital of Stomatology, National Engineering Laboratory for Digital and Material Technology of Stomatology, Research Center of Engineering and Technology for Digital Dentistry of Ministry of Health, Beijing Key Laboratory of Digital Stomatology, Beijing, China.

^bProfessor, Center of Digital Dentistry, Department of Prosthodontics, Peking University School and Hospital of Stomatology, National Engineering Laboratory for Digital and Material Technology of Stomatology, Research Center of Engineering and Technology for Digital Dentistry of Ministry of Health, Beijing Key Laboratory of Digital Stomatology, Beijing, China.

^cProfessor, Center of Digital Dentistry, Department of Prosthodontics, Peking University School and Hospital of Stomatology, National Engineering Laboratory for Digital and Material Technology of Stomatology, Research Center of Engineering and Technology for Digital Dentistry of Ministry of Health, Beijing Key Laboratory of Digital Stomatology, Beijing, China.

^dAssistant Professor, Center of Digital Dentistry, Department of Prosthodontics, Peking University School and Hospital of Stomatology, National Engineering Laboratory for Digital and Material Technology of Stomatology, Research Center of Engineering and Technology for Digital Dentistry of Ministry of Health, Beijing Key Laboratory of Digital Stomatology, Beijing, China.

Clinical Implications

Powder-free intraoral scanning should be used with care for scanning high-translucency tooth structure or dental materials. The use of a suitable measurement method such as powder or software compensation should be considered.

object is subsequently emitted at a different point and at a different angle than it would have had it been reflected directly off the surface. SSS light contaminates the measurements of directly reflected surface light detected by the charge-coupled device sensor of an intraoral scanning system, thus reducing the accuracy of its resulting datasets.⁶ Previous studies^{7,8} have described the use of silicon dioxide powder with intraoral scanning systems to limit this problem, albeit with the possibility of added inaccuracies due to overlapped spray.⁹ Contemporary intraoral scanners designed on the principle of confocal measurement,^{10,11} as used in this study, allow for the capture of intraoral tissue morphology without the need for powder. Modern dental ceramics exhibit the major translucent optical properties of natural teeth.¹² The use of such translucent dental materials with a confocal system has not yet been analyzed. A recent study measured the height of nine 2-mm-thick material specimens (ceramic, composite resin, and metal), and calculated the differences between the surfaces of the test specimens and the reference enamel specimen.¹³ However, the object tested was a flat plane; the scanning accuracy of a translucent preparation shaped object should also be tested. Some studies have suggested that scanning accuracy is relative to the refractive index, translucency parameter, but with only 1 kind of translucent material or lots of materials with the same shade (A2).^{13,14} To date, the relationship between translucency and scanning accuracy has still not been determined. In dental color science, the translucency parameter and contrast ratio (CR) are often used to assess the translucency of a material.¹³ Translucency describes the color difference between a material with a black backing and that with a white one. Contrast ratio is the ratio of the reflectance of a specimen over a black backing to that over a white backing. Neither of them can assess the influence of SSS light. In this study, parameters refer to different parts of incident light were used: R refers to the reflected light, T refers to the transmitted light, and S+A refers to the residual part of the light.

To evaluate the 3-dimensional (3D) scanning error of the intraoral scanner, a limited number of studies have used the definitions of "accuracy,"^{7,8,15-20} which includes both "trueness" and "precision." According to International

Organization for Standardization (ISO) standard 5725,²¹ the measure of trueness is usually expressed in terms of "bias," which refers to the total systematic error of a measuring method. The measurement of precision is usually expressed in terms of "imprecision," computed as a standard deviation of the test results and depends solely on the distribution of random errors. With this method, however, local differences cannot be reflected. Previous studies have displayed different distributions with a color map.^{15,22,23} Taking this technique one step farther, measurements in cross-sections are needed to describe localized misfit for supplementing trueness.

The purpose of this *in vitro* study was to assess the influence of object translucency on powder-free intraoral scanning accuracy by using offset copings of serial translucent ceramics fabricated from the same datasets. Primary sintered zirconia was used as the control. The null hypothesis was that object translucency would not influence the scanning accuracy of the tested powder-free intraoral scanner.

MATERIAL AND METHODS

Six 1.00-mm-thick, lightness gradually decreasing, rectangle-shaped ceramic specimens (12- ×10- mm CEREC Blocs; S0-M to S5-M; lot number 21490; Sirona) were sliced with a diamond wire saw (product STX-202; Shenyang Kejing Auto-instrument Co, Ltd). Spectral transmittance and reflectance in the wavelength of visible light (360 to 780 nm) under standard illuminant D65 were obtained at 10-nm intervals (n=43) by using a computer-controlled spectrophotometer (Color-Eye 7000A; X-Rite) with a 1-nm spectral resolution. Three translucency related parameters were calculated based on these data according to the studies of Shiraishi et al²⁴ and Friebel et al.²⁵ The average reflectance with black backing (R_b) was defined as the mean of the 43 spectral reflectance data, which refers to all light detected by the scanning system, including reflected light and SSS light. The average transmittance (T) was defined as the mean of the 43 spectral transmittance data, which refers to light that passes through the specimen. The percentage sum of scattering (S) and absorption (A) refers to the light of the residual part (computational formula: $S+A=100\% - R_b - T$). Similar to that in dental hard tissues, absorption is typically much lower than scatter.²⁶ Therefore, S+A mostly represents the light scattered inside the material. All parameters related to translucency in this study were percentages of the incident light.

A 1.00-mm offset coping with a shoulder collar (finish line configuration of 90 degrees) of a prepared right maxillary first molar was designed by using computer-aided design (CAD) software (inLab; product 4.2.5.82936; Sirona). One primary sintered zirconia coping and 6 ceramic copings were fabricated with the

Table 1. Settings for 2 different CAD-CAM materials according to CEREC specifications

Parameter	Ceramic Blocks	Primary Sintered Zirconia
CAD		
Thickness, μm	1000	1000
Cement spacer, μm	0	0
Above margin, μm	300	300
Considering pin shape	No	No
Remove undercut	No	No
Diameter of the pin, mm	$D_1=1.7$	$D_2=1.3$
Batch no.	21490	2013298238

CAD, computer-aided design.

same dataset by using a 3-axis computerized numerical control milling machine (CEREC XL premium package; Sirona). Table 1 shows the settings for both CAD and computer-aided manufactured (CAM) materials. A standard base was designed by using dimensional reverse engineering software (Geomagic Studio; 3D Systems) and fabricated by using a high-precision 5-axis computerized numerical control milling machine (Zenotech Ti; nominal accuracy $\pm 10 \mu\text{m}$; Wieland Dental). Bases were made of white wax-resin (Organic; R+K CAD/CAM Technologie, GmbH & Co KG) with a "preparation" in the center to locate the offset coping. Figures of spheres were distributed around the preparation to offer curvature characteristics to decrease the 3D image mismatch and establish proper measurement coordinates. Each coping was placed onto the base with its inside surfaces painted black, axially loaded with finger pressure²⁷ until a noneugenol interim cement (Meta Biomed Co Ltd) had set, and examined for any visible gap around the coping margin.

An intraoral scanner designed on the basis of confocal measurement principle (Organic; R+K CAD/CAM Technologie, GmbH & Co KG) was used. Scanning began at the center of the occlusal surface and then radiated outward toward the periphery along the radial lines (Fig. 1). Every part of the surface was scanned at a 90-degree angle to obtain 3D shape datasets of a specimen in stereolithography (STL) format. Data with obvious faults (for example, double layers or missing data) were excluded. Each offset coping was scanned 5 times. All datasets were imported in a 3D metrology software (Geomagic Qualify 2013 inspection; 3D Systems) for analysis. The upside of the base and the outside of the offset copings areas were reserved, including the collar while excluding the connected pole. The upper base area was used for 3D shape dataset alignment, and the coping area was for scanning accuracy evaluation. If the precision of the base alignment process satisfied the assumption of less than 0.010 mm, then the evaluation of scanning accuracy began.

The scanning precision of each of the 7 specimens was evaluated separately. Among the 5 3D shape

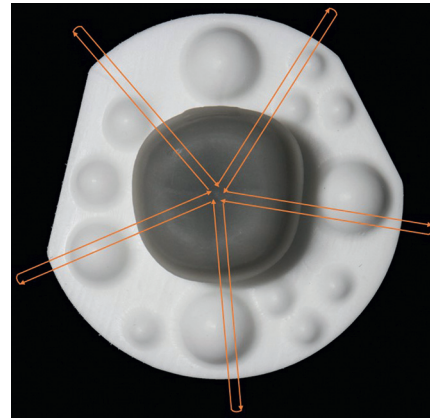


Figure 1. Scanning route.

datasets of a specimen, 1 was randomly selected as a reference dataset (ref-datum) by using "Data-Select Cases-Random sample of cases" order in SPSS software, and the remaining specimens ($n=4$) were regarded as test datasets (test-data). The field of all test-data was the same and was modified to be slightly smaller than that of the ref-datum. Then, 1 test-datum was superimposed on the ref-datum by using the "best fit alignment" tool of a report and a 3D comparison analysis histogram spectrum was exported. The report exported 4 parameters: mean (mm), positive mean (mean+, mm), negative mean (mean-, mm), and standard deviation (SD, mm) of the 3D deviation. The mean value related to the whole coping area and indicated the superiority of positive or negative errors. Mean+ related to the mean error of area that the test-data above the ref-data. Mean- related to the mean error of area that the test-data beneath the ref-data. SD shows the fluctuation of 3D deviation within a test-datum. The remaining 3 test data were analyzed similarly. The mean \pm SD of the 4 means, means+ and means- of the specimen were defined as the scanning imprecision of the specimen.

The scanning trueness of the specimens of the 6 translucency gradient changing ceramic copings were evaluated separately in a similar process. One primary sintering offset coping 3D shape dataset was randomly selected as ref-datum in the same way mentioned above. Five 3D shape datasets of each ceramic offset coping were regarded as test-data. The mean \pm SD of the 5 means, means+ and means- of a specimen were defined as the scanning bias of the specimen.

For the cross-sectional difference measurement of the specimens of 6 translucency gradient changing ceramic copings, the same ref-datum and 1 test-datum of each specimen for scanning bias evaluation were used for the second time. A measurement of the coordinate system was established based on the 3 largest feature spheres on the base of the ref-datum. Specifically, the x-, y-, and

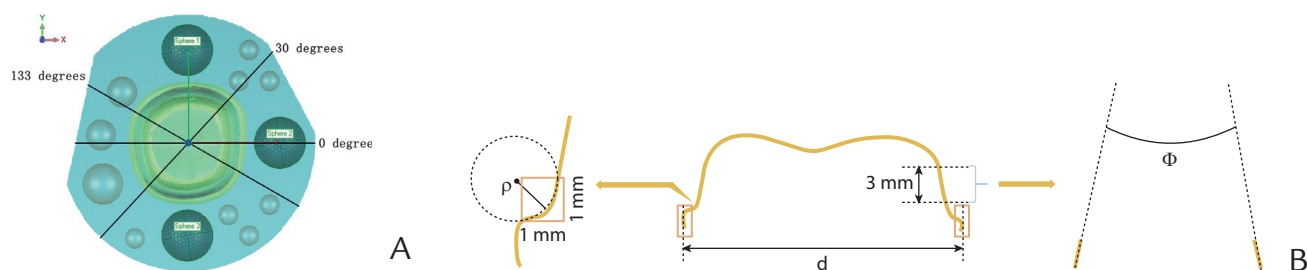


Figure 2. Measurement of cross-sectional differences. A, Coordination construction and cross-section selection. B, Measurement diagram of cross-section. Coping diameter (d): largest horizontal distance of offset coping collar; convergence angle (Φ): angle of convergence between middle one-third of opposite axial walls; curvature radius (ρ): of internal gingivoaxial corner of offset coping collar (area of 1×1 mm).

z-axis referred to the mesial-distal direction, labial-lingual direction, and location direction relative to the coping in the center. After the base alignment process, 3 cross-sections (rotation angle from positive direction of x -axis: 0 degree, 30 degrees, and 133 degrees) were made. In each cross-section, 3 parameters were defined as follows (Fig. 2): coping diameter (d , mm), meaning the largest horizontal distance of the collar of the offset coping; convergence angle (Φ , degree), meaning the angle of convergence between the middle one-third of the opposite axial walls; and curvature radius (ρ , mm), meaning the internal gingivoaxial corner of the offset coping collar (measuring area of 1×1 mm). Mean differences of each parameter (Δd , $\Delta \Phi$, $\Delta \rho$) in each cross-section between ref-datum and test-datum were measured to evaluate the cross-sectional difference of each specimen.

The normality of data distribution was tested by using the Kolmogorov-Smirnov and Shapiro-Wilk tests. One-way ANOVA based on the assumption of normal data distribution was used to analyze the parameters of scanning accuracy (bias, imprecision, Δd , $\Delta \Phi$, and $\Delta \rho$) among 6 ceramic offset copings, and post hoc comparisons were made by using the Tukey honest significant difference test separately. Bivariate correlation was used to analyze the relationships between each parameter of scanning accuracy (bias, imprecision, Δd , $\Delta \Phi$, and $\Delta \rho$) and translucency (R_b , T , and $S+A$) ($\alpha=.05$).

RESULTS

Figure 3 shows the typical curves of spectral reflectance and transmittance data of dental ceramics. The reflectance and transmittance of ceramic blocs from S0-M to S5-M in the short wavelength range (approximately 580 nm) systematically decreased. No obvious differences were found in reflectance between S1-M and S2-M, and S0-M exhibited a less variable pattern of transmittance than the others. Optical parameter data for R_b , T , and $S+A$ are shown in Table 2.

The imprecision of the base alignments was 0.000 ± 0.002 mm. The 3D deviation of the third 3D shape

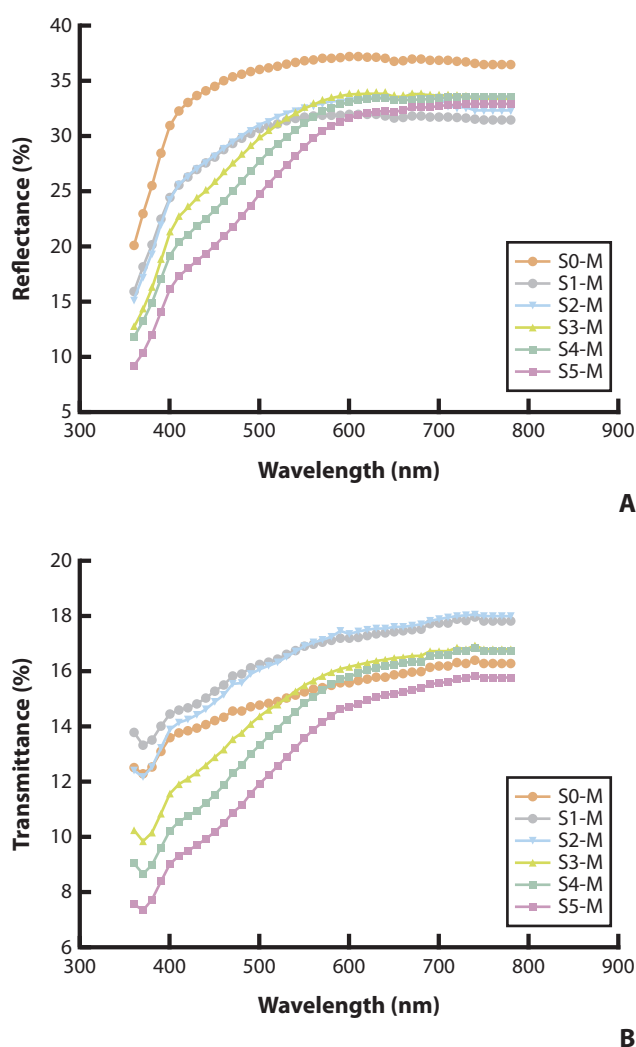


Figure 3. Spectral reflectance. A, Transmittance. B, Curves for slice specimens ranging from S0-M to S5-M. Both spectral reflectance and transmittance showed serial decrease in relatively short wavelengths (360-580 nm). S1-M and S2-M showed similar reflectance but different transmittance values. S0-M exhibited spectral transmittance.

dataset of S5-M was checked as an outlier by drawing a box plot and deleted. The scanning imprecisions of the 7 specimens are given in Figure 4 and Table 3.

Table 2. Optical parameters related to translucency of each ceramic slice

Ceramic Slice	R _b (%)	T (%)	S+A (%)
S0-M	34.55	14.06	51.39
S1-M	28.79	15.97	55.24
S2-M	29.59	15.37	55.04
S3-M	28.44	14.37	57.19
S4-M	26.86	13.67	59.47
S5-M	26.20	13.12	60.68

R_b, average reflectance of ceramic slices with black backing; S+A, percentage sum of scattering (S) and absorption (A); T, average transmittance of ceramic slices.

Table 3. Scanning bias of each ceramic copings

Ceramic Coping	Bias (mm)		
	Mean ±SD	Mean ±SD	Mean ±SD
S0-M	0.149 ±0.038	0.149 ±0.038	-0.005 ±0.002
S1-M	0.132 ±0.038	0.148 ±0.022	-0.018 ±0.010
S2-M	0.103 ±0.039	0.107 ±0.036	-0.015 ±0.009
S3-M	0.117 ±0.038	0.120 ±0.038	-0.013 ±0.006
S4-M	0.073 ±0.039	0.079 ±0.035	-0.016 ±0.110
S5-M	0.068 ±0.020	0.072 ±0.018	-0.010 ±0.001

Mean, average deviations of whole coping area; Mean+, average deviations of area that test data above reference data; Mean-, average deviations of area that test data beneath the reference data; SD, fluctuation of 3-dimensional deviation within test datum.

The scanning biases of the 6 translucent copings are shown in Figure 5 and Table 4. A significant difference in both mean+ and mean of bias was found among 6 translucent copings ($P < .05$), and a difference exists between S0-M and S4-M and between S0-M and S5-M ($P < .05$). Figure 6 shows the 3D comparison analysis histogram spectrum of each specimen, with the major area showing a positive deviation, a negative difference mainly distributed around the finish line area of the coping, and minimal difference in the middle of the axial wall.

Mean ±SD of 2D cross-section difference (Δd , $\Delta\Phi$, $\Delta\rho$) between ceramic and zirconia copings measured in 3 cross-sections are given in Figure 7 and Table 5. 3D shape datasets of ceramic copings showed a smaller mean diameter ($\Delta d = -0.067$ mm), larger convergence angle ($\Delta\Phi = 2.79$ degrees), and larger curvature radius ($\Delta\rho = 0.236$ mm). The morphology change of the internal gingivoaxial corner is given in Figure 8. No significant differences were found among the 6 ceramic offset copings (Δd : $P = .444$; $\Delta\Phi$: $P = .857$; $\Delta\rho$: $P = .828$).

Significant correlation existed between S+A and the mean of scanning bias ($P < .01$), S+A and mean+ of scanning bias ($P < .05$), as well as between R_b and mean of scanning bias ($P < .05$). Additionally, $\Delta\rho$ measurement of cross-sectional difference was significantly associated with S+A ($P < .01$). Details are given in Table 6.

DISCUSSION

Results of this study do not support the null hypothesis that object translucency would not influence the scanning accuracy of the tested powder-free intraoral scanner. The

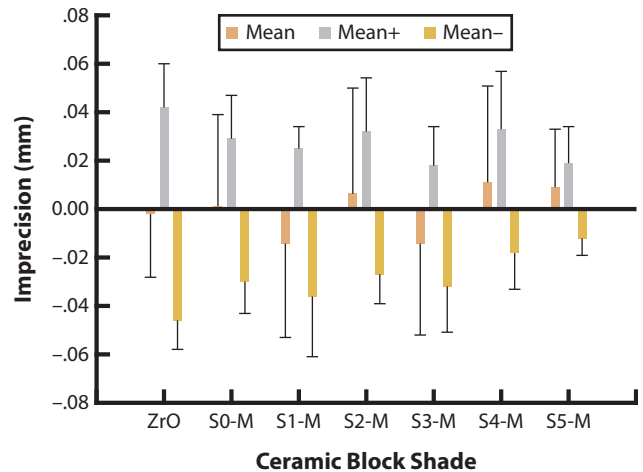


Figure 4. Imprecision of six ceramic offset copings. Means and standard deviations are shown.

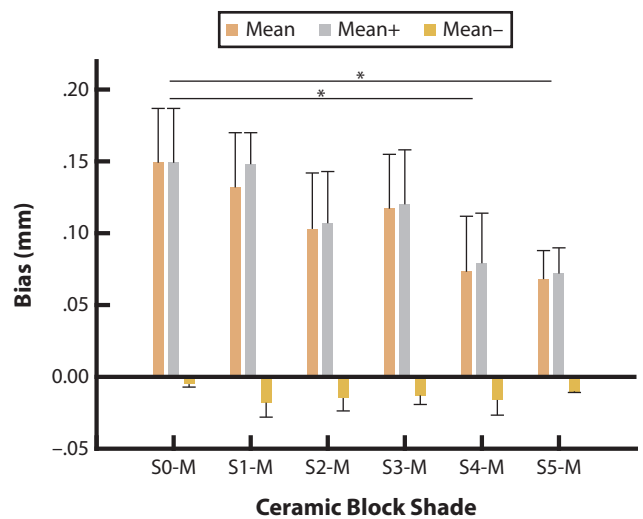


Figure 5. Bias of six ceramic offset copings. Means and standard deviations are shown. *Significant difference was found between S0-M and S4-M, S0-M and S5-M ($P < .05$).

Table 4. Scanning imprecision of each coping

Coping	Imprecision (mm)		
	Mean ±SD	Mean ±SD	Mean ±SD
ZrO	-0.002 ±0.026	0.042 ±0.018	-0.046 ±0.012
S0-M	0.001 ±0.038	0.029 ±0.018	-0.030 ±0.013
S1-M	-0.014 ±0.039	0.025 ±0.009	-0.036 ±0.025
S2-M	0.006 ±0.044	0.032 ±0.022	-0.027 ±0.012
S3-M	-0.014 ±0.038	0.018 ±0.016	-0.032 ±0.019
S4-M	0.011 ±0.040	0.033 ±0.024	-0.018 ±0.015
S5-M	0.009 ±0.024	0.019 ±0.015	-0.012 ±0.007

Mean, average deviations of whole coping area; Mean+, average deviations of area that test data above reference data; Mean-, average deviations of area that test data beneath the reference data; SD, fluctuation of 3-dimensional deviation within test datum; ZrO, zirconium(II) oxide.

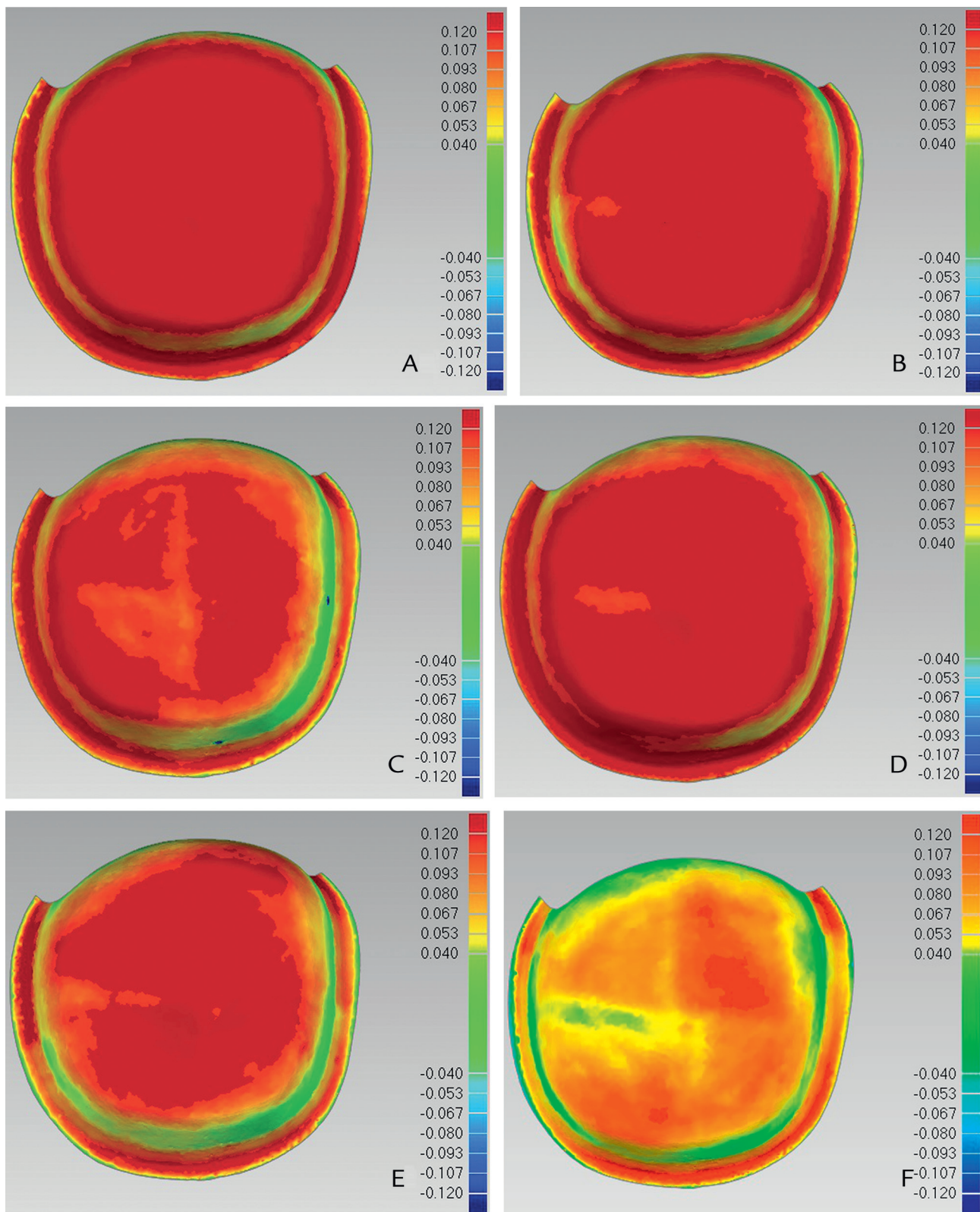


Figure 6. Difference color map of bias measurement. One coping with median bias value of each specimen. A, S0-M. B, S1-M. C, S2-M. D, S3-M. E, S4-M. F, S5-M. Deviation spectrum was set from -0.120 to 0.120 mm. Maroon areas refer to areas beyond ± 0.120 mm.

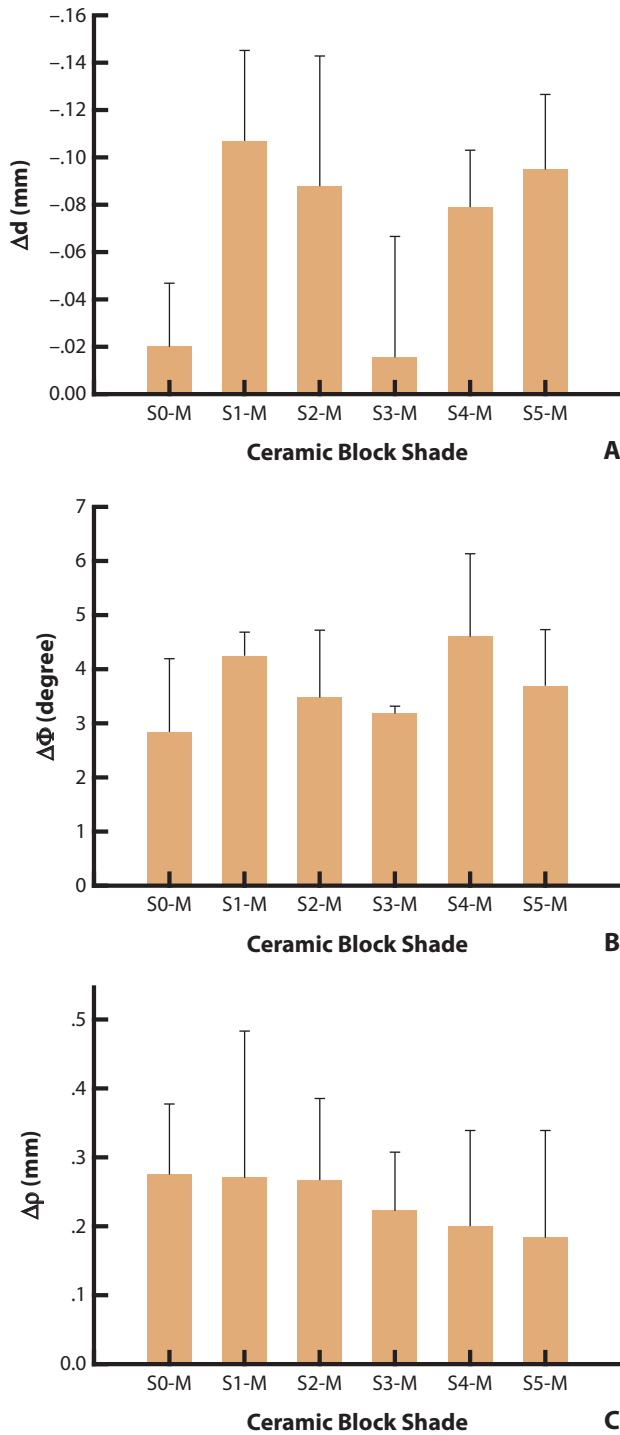


Figure 7. Means of coping diameter difference (A, Δd), convergence angle difference (B, $\Delta\Phi$), and curvature radius difference (C, $\Delta\rho$) of all specimens in three cross-sections.

scanner used in this study was designed on the basis of the principle of confocal measurement, which should theoretically counteract the influence of translucence¹⁴ by detecting the surface shape layer by layer or point by point, thus leading to a lower scanning efficiency.

Table 5. Means of 2D cross-section differences between ceramic and zirconia copings

Ceramic coping	Δd (mm), Mean \pm SD	$\Delta\Phi$ (degree), Mean \pm SD	$\Delta\rho$ (mm), Mean \pm SD
S0-M	-0.020 \pm 0.027	2.838 \pm 1.353	0.275 \pm 0.102
S1-M	-0.107 \pm 0.038	4.255 \pm 0.430	0.270 \pm 0.213
S2-M	-0.088 \pm 0.055	3.488 \pm 1.233	0.267 \pm 0.119
S3-M	-0.016 \pm 0.051	3.183 \pm 0.136	0.222 \pm 0.085
S4-M	-0.079 \pm 0.024	4.603 \pm 1.531	0.200 \pm 0.139
S5-M	-0.095 \pm 0.032	3.695 \pm 1.036	0.183 \pm 0.156

2D, two-dimensional; Δd , coping diameter difference; $\Delta\Phi$, convergence angle difference; $\Delta\rho$, curvature radius difference.

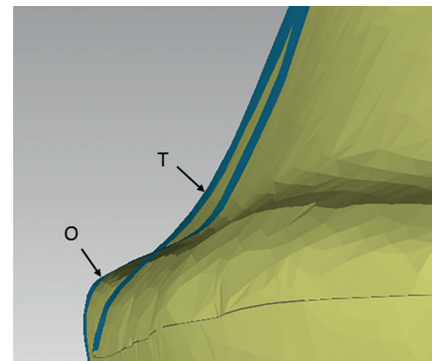


Figure 8. Morphology change of internal gingivoaxial corner of ceramic offset coping. Opaque primary sintering zirconia offset coping (O) showed clear internal gingivoaxial corner while translucent ceramic offset coping (T) lost curvature features.

Measurement errors tend to appear as displacement and curvature at the corner tend to decrease.

In this study, a significantly large positive bias (S0-M to S5-M: 0.149 \pm 0.038 mm to 0.068 \pm 0.020 mm) of translucent offset copings was found, which is a trend similar to that found by Nedelcu et al.⁹ Offset copings made of ceramic blocks of larger translucency showed a larger bias ($P < .05$), which means different translucent materials will deviate and deform the preparation. The reasons can be analyzed as follows. As the contaminant light originated from the subsurface layer, the bias was suggested to be negative. However, the mean bias in this study was positive. The first assumption is that the powder-free intraoral scanning system software is thought to create an internal correction value for counteracting measurement bias in this situation, even though the results of this correction are not clinically acceptable. Second, the influence of the specific base should also be analyzed. Previous studies analyzed the scanning accuracy of different scanners by using a standard model,^{7,15,22} whereas other studies judged different digital modeling methods with the same scanner.^{28,29} In these examples, the same area may be used for both registration and measurement. In the present study, even when scanning the offset copings of

Table 6. Correlation coefficients (*r*) among bias and optical parameters

Parameter	R _b (%)	T (%)	S+A (%)
Bias			
Mean			
<i>r</i>	0.843 ^a	0.556	-0.918 ^b
<i>P</i>	0.035	0.252	0.010
Mean+			
<i>r</i>	0.736	0.648	-0.877 ^a
<i>P</i>	0.078	0.164	0.022
Mean-			
<i>r</i>	0.605	-0.565	-0.354
<i>P</i>	0.203	0.243	0.491
Imprecision			
Mean			
<i>r</i>	-0.173	-0.594	0.341
<i>P</i>	0.743	0.214	0.509
Mean+			
<i>r</i>	-0.347	-0.560	0.483
<i>P</i>	0.501	0.247	0.332
Mean-			
<i>r</i>	-0.540	-0.801	0.730
<i>P</i>	0.269	0.055	0.100
Cross-sectional difference			
Δd			
<i>r</i>	0.566	-0.273	-0.412
<i>P</i>	0.241	0.600	0.417
ΔΦ			
<i>r</i>	0.418	0.392	-0.492
<i>P</i>	0.410	0.442	0.321
Δρ			
<i>r</i>	0.784	0.772	-0.935 ^b
<i>P</i>	0.065	0.072	0.006

Δd, coping diameter difference; ΔΦ, convergence angle difference; Δρ, curvature radius difference; R_b, average reflectance of ceramic slices with black backing; S+A, percentage sum of scattering (S) and absorption (A); T, average transmittance of ceramic slices. ^aSignificant at *P*<.05. ^bSignificant at *P*<.01.

the same surface morphology measured by the same scanner, various translucencies might affect the scanning outcomes; thus, a specific opaque base offering common regions for dataset registration is necessary. To obtain the complete morphology of the offset coping, the base should be low in case of impeding measuring light. As a result, the registration area was relatively lower than the test area. When the coping specimen was scanned, the occlusal plane and upside surface of the base were scanned at the same time. Combining these specific experimental conditions, the use of the base produced 2 factors that may contribute to scanning bias. First, at an unsuitable depth of focus, the quality of measurement will decrease. Second, when the registration area is far from the test area, the value of scanning bias will be relatively larger. As the operation is unified, the effect of the base will be the same for all coping digitalization processes.

Translucent offset copings showed a curvature decrease on a surface with large curvature (small curvature radius).

In other words, the curvature radius becomes larger (positive Δρ, *P*<.05), specifically, sharp corners become more rounded. Because the preparation finish line is sharp, at the extreme, with a 90-degree finish line corner, an increase of ρ makes the offset coping collar slightly narrower (Δd=-0.067 mm). Considering the difference of pin diameters (0.2 mm) between objects, highly translucent specimens (S0-M to S3-M) showed larger Δρ values (Δρ=0.236 mm). As a result, the convergence angle becomes larger (ΔΦ=2.79 degrees). With this dataset, the prosthesis will be difficult to locate, and the shoulder of the crown will be shorter, thus forming a step. To solve this problem, a suitable margin compensation, such as lengthening the restoration margin, should be added during the CAD process. Increasing Φ is another integrated representation of Δρ, which increases the difficulty of seating the restoration. The spheres on the base helped decrease the error associated with the registration calculation of the offset coping axial wall during scanning, as mismatched data would be corrected when the central coping and figure spheres are maintained with the scan wand in the same field of view for several seconds. However, the trend of change of Φ and d without the spheres is unclear. Future studies will address this topic. From S0-M to S5-M, R_b and T decreased, whereas S+A increased, which is a result similar to that of Shiraiishi et al.²⁴ Significant correlation existed between S+A and mean values (*P*<.01), S+A and mean+ values (*P*<.05), and between R_b and mean values (*P*<.05). The total light reflected on a surface, scattered inside the material, and then emitted from the material (SSS light) is detected as a whole, which can be represented by R_b. The emitted SSS light produces most measurement errors,^{6,30-33} and SSS light, or the maximum response of a laser or light beam striking a translucent surface as seen by a camera is often below the actual surface.³¹ Furthermore, the amount of SSS light is related to the inner structure of the measured object, so the optical parameter S+A, which is affected by the material's inner features, has the largest correlation with measurement bias in this study.

As translucency varies, even within a single natural tooth,³⁰ the difference of bias could be another source of morphological change. In contrast, as the range of translucency is limited in tissues of the human tooth, the influence of translucent materials is not so sensitive. A significant difference of displacement occurs with higher translucency objects (greater translucency than S1-M/A1C), and curvature decrease occurs on all translucent materials. Different translucent ceramic coping showed no obvious difference in scanning deformation. However, in this study, only glass ceramics were evaluated. As figures of translucency of material are closely influenced by their interior structure, more clinical prosthetic materials should be tested.

In addition, different scanning principles for the powder-free intraoral scanner are available now. Jeon et al³⁴ found that repeatability (mean \pm SD) of a blue-light scanner was smaller than the white-light one. Thus illustrate that scanning principle will be a key factor of scanning accuracy of powder-free scanners. Whether the influence of objective translucency is similar to the scanning accuracy of other powder-free intraoral scanners needs to be further elucidated.

CONCLUSIONS

Using the tested powder-free intraoral scanner, higher translucency objects (greater translucency than S1-M/A1C) resulted in lower scanning accuracy and larger morphological changes. Therefore, more suitable methods of measurement are still required.

REFERENCES

- Logozzo S, Franceschini G, Kilpelä A, Caponi M, Governi L, Blois L. A comparative analysis of intraoral 3D digital scanners for restorative dentistry. *Internet J Med Technol* 2001;5.
- Birnbaum NS, Aaronson HB, Stevens C, Cohen B. 3D digital scanners: A high-tech approach to more accurate dental impressions. *Inside Dent* 2009;5.
- Harrison L. Digital impressions competition booming. 2009. Available at: <http://www.drbcusp.com/index.aspx?sec=ser&sub=def&pag=dis&ItemID=301650>. Last accessed July 6, 2016.
- D'Apuzzo N. Overview of 3D surface digitization technologies in Europe. *Proc SPIE Int Soc Opt Eng* 2006;6056:5605-17.
- Xiong F, Chao Y, Zhu Z. Translucency of newly extracted maxillary central incisors at nine locations. *J Prosthet Dent* 2008;100:11-7.
- Nayar SK, Krishnan G, Grossberg MD, Raskar R. Fast separation of direct and global components of a scene using high frequency illumination. *ACM Transactions on Graphics (TOG)* 2006;25:935-44.
- Patzelt SB, Emmanouilidi A, Stampf S, Strub JR, Att W. Accuracy of full-arch scans using intraoral scanners. *Clin Oral Investig* 2014;18:1687-94.
- Andriessen FS, Rijkens DR, van der Meer WJ, Wismeijer DW. Applicability and accuracy of an intraoral scanner for scanning multiple implants in edentulous mandibles: a pilot study. *J Prosthet Dent* 2014;111:186-94.
- Nedelcu RG, Persson AS. Scanning accuracy and precision in 4 intraoral scanners: an in vitro comparison based on 3-dimensional analysis. *J Prosthet Dent* 2014;112:1461-71.
- Henkel GL. A comparison of fixed prostheses generated from conventional vs digitally scanned dental impressions. *Compend Contin Educ Dent* 2007;28:422-4.
- NS Birnbaum, Aaronson HB. Dental impressions using 3D digital scanners: virtual becomes reality. *Compend Contin Educ Dent* 2008;29:494-505.
- Winkler D. Fundamentals of color: Shade matching and communication in esthetic dentistry. *Br Dent J* 2005;199:59.
- Kurz M, Attin T, Mehl A. Influence of material surface on the scanning error of a powder-free 3D measuring system. *Clin Oral Investig* 2015;19:2035-43.
- Keul C, Stawarczyk B, Erdelt KJ, Beuer F, Edelhoff D, Güth JF. Fit of 4-unit FDPs made of zirconia and CoCr-alloy after chairside and labside digitalization—a laboratory study. *Dent Mater* 2014;30:400-7.
- Ender A, Mehl A. Accuracy of complete-arch dental impressions: a new method of measuring trueness and precision. *J Prosthet Dent* 2013;109:121-8.
- Wiranto MG, Engelbrecht WP, Tutein Nolthenius HE, van der Meer WJ, Ren Y. Validity, reliability, and reproducibility of linear measurements on digital models obtained from intraoral and cone-beam computed tomography scans of alginate impressions. *Am J Orthod Dentofacial Orthop* 2013;143:140-7.
- Flügge TV, Schlager S, Nelson K, Nahles S, Metzger MC. Precision of intraoral digital dental impressions with iTero and extraoral digitization with the iTero and a model scanner. *Am J Orthod Dentofacial Orthop* 2013;144:471-8.
- Patzelt SB, Vonau S, Stampf S, Att W. Assessing the feasibility and accuracy of digitizing edentulous jaws. *J Am Dent Assoc* 2013;144:914-20.
- Naidu D, Freer TJ. Validity, reliability, and reproducibility of the iOC intraoral scanner: a comparison of tooth widths and Bolton ratios. *Am J Orthod Dentofacial Orthop* 2013;144:304-10.
- Nayyar N, Yilmaz B, McGlumphy E. Using digitally coded healing abutments and an intraoral scanner to fabricate implant-supported, cement-retained restorations. *J Prosthet Dent* 2013;109:210-5.
- Zhongning W, Zhimin L, Xintao X, Lianqing Zh. Evaluation of measurement error and uncertainty. 1st ed. Beijing: Science Press; 2008:49-50.
- Ender A, Mehl A. Full arch scans: conventional versus digital impressions—an in-vitro study. *Int J Comput Dent* 2011;14:11-21.
- Hasegawa A, Ikeda I, Kawaguchi S. Color and translucency of in vivo natural central incisors. *J Prosthet Dent* 2000;83:418-23.
- Shiraishi T, Wood DJ, Shinozaki N, van Noort R. Optical properties of base dentin ceramics for all-ceramic restorations. *Dent Mater* 2011;27:165-72.
- Friebel M, Povel K, Cappius HJ, Helfmann J, Meinke M. Optical properties of dental restorative materials in the wavelength range 400 to 700 nm for the simulation of color perception. *J Biomed Opt* 2009;14:54029.
- Chen QG, Lin B. Optical penetration depth simulation of dental tissue based on finite element method. *Acta Photonica Sinica* 2010;39:680-3.
- Weaver JD, Johnson GH, Bales DJ. Marginal adaptation of castable ceramic crowns. *J Prosthet Dent* 1991;66:747-53.
- Rungruanganunt P, Kelly JR, Adams DJ. Two imaging techniques for 3D quantification of pre-cementation space for CAD/CAM crowns. *J Dent* 2010;38:995-1000.
- Conrad HJ, Delong R. Accuracy of two impression techniques with angulated implants. *J Prosthet Dent* 2007;97:349-56.
- Baum K, Hartmann R, Bischoff T, Oelerich JO, Finkensieper S, Heverhagen JT. Three-dimensional surface reconstruction within noncontact diffuse optical tomography using structured light. *J Biomed Opt* 2012;17:126009.
- Holroyd M, Lawrence J. An analysis of using high-frequency sinusoidal illumination to measure the 3D shape of translucent objects. *IEEE Comput Vis Pattern Recognit* 2011:2985-91.
- Tongbo C, Lensch H, Fuchs C, Seidel HP. Polarization and phase-shifting for 3D scanning of translucent objects. *Proc IEEE Comput Soc Conf Comput Vis Pattern Recognit* 2007:1987-94.
- Narasimhan SG, Nayar SK, Bo S, Koppal SJ. Structured light in scattering media. *IEEE I Conf Comp Vis* 2005:420-7.
- Jeon JH, Choi BY, Kim CM, Kim JH, Kim HY, Kim WC. Three-dimensional evaluation of the repeatability of scanned conventional impressions of prepared teeth generated with white- and blue-light scanners. *J Prosthet Dent* 2015;114:549-53.

Corresponding author:

Dr Peijun Lyu
Center of Digital Dentistry
Peking University School and Hospital of Stomatology
22 Zhongguancun Nandajie, Haidian District, Beijing 100081
CHINA
Email: kqlpj@bjmu.edu.cn

Acknowledgments

The authors thank Dr Ningfang Liao and graduate student Yasheng Li from Color Science and Engineering Lab of Beijing Institute of Technology for assistance with the optical parameter measurements.

Copyright © 2016 by the Editorial Council for *The Journal of Prosthetic Dentistry*.